ELSEVIER

Biophysical Chemistry 105 (2003) 461–470

Biophysical Chemistry

www.elsevier.com/locate/bpc

Vibrational and electronic couplings in ultraviolet resonance Raman spectra of cyclic peptides☆

Yang Wang[a], Thomas G. Spiro[b,*]

[a]*Bioprocess Medical Research, Merck Research Laboratory, West Point, PA 19486, USA*
[b]*Department of Chemistry, Princeton University, Princeton, NJ 08544, USA*

Received 23 October 2002; received in revised form 17 December 2002; accepted 17 December 2002

Abstract

Ultraviolet resonance Raman (UVRR) spectra are reported for a series of cyclic amides. 2-Azacyclotridecone, which has a 13-membered ring, shows a classic *trans*-amide UVRR spectral pattern, with comparable enhancement of the amide modes II, III and S. When the ring is diminished to eight (ε-caprolactam) or seven (2-azacyclooctanone) members, this pattern is replaced by a single strong band near 1497 cm^{-1}, characteristic of the C–N stretch of a *cis*-amide vibration (amide IIc). Further shrinkage of the ring decreases the amide IIc frequency. It is lowered over 100 cm^{-1} to 1389 cm^{-1} in the case of a 4-membered ring (2-azaidine), reflecting diminution of the C–N bond order due to ring strain and pyramidalization of the C and N atoms. At the same time the amide Ic (C=O stretching) frequency increases, reflecting the localization of the C=O double bond. Also the sensitivity to hydrogen–deuterium exchange reverses for amide Ic and IIc modes as ring size decreases. The UV absorption maximum, which is red-shifted for *cis*-relative to *trans*-amides, shifts increasingly to the blue as the ring size decreases, again reflecting localization of the π bonding. In the case of amides with 5- and 6-membered rings (2-pyrrolidinone and δ-vareloctam) multiple UVRR bands are seen in the amide IIc region, whose relative intensities are temperature-dependent. These are assigned to conformers in which different members of the ring are out of the mean plane, resulting in variable perturbations of the amide bond. The cyclic dipeptides cyclo(Gly–Gly) and cyclo(Gly–Pro) have perturbed amide IIc frequencies, reflecting the kinematic mixing of the amide coordinates into in- and out-of-phase modes. Excitation profiles reveal electronic mixing as well, with the transition dipoles adding for the in-phase and canceling for the out-of-phase modes.

Keywords: Ultraviolet resonance Raman; C–N stretch; Ring strain; Cyclic peptides; Amide

☆ Dedicated to Walter Kauzman, a career-long friend and inspiration

*Corresponding author. Tel.: +1-609-258-3907; fax: +1-609-258-0348.
E-mail address: spiro@princeton.edu (T.G. Spiro).

0301-4622/03/$ - see front matter © 2003 Elsevier Science B.V. All rights reserved.
doi:10.1016/S0301-4622(03)00108-X

1. Introduction

The ultraviolet resonance Raman (UVRR) spectroscopy of the amide bond has attracted much interest because the technique offers a probe of the secondary and tertiary structures in proteins [1–4]. An important characteristic is that the UVRR spectrum is greatly altered upon conversion of the *trans*-peptide bond to the *cis*-peptide isomer, or upon replacement of the N-bound H atom with either deuterium or a carbon substitution, as in peptidyl–proline bonds. For a normal *trans*-peptide bond one observes strong UV enhancement of three characteristic Raman the classic amide II ($\sim$1570 cm^{-1}) and amide III ($\sim$1300 cm^{-1}) bands, while enhancement of amide I (C=O stretching) is weak [5]. Enhancement of another mode, characterized as amide S [6] (for structure sensitive) or (C)C_αH bending [7] depends on the peptide dihedral angles, [5,6] and is absent in *cis*-peptide spectra [8]. The amide II and III modes are mainly in- and out-of-phase combinations of the C–N stretching and N–H bending coordinates; [9] this coordinate mixing is eliminated when the N-bound H atom is replaced by a heavier atom. Only a single strong UVRR band near 1500 cm^{-1}, arising mainly from C–N stretching, is seen upon N–H/D exchange (when it is called amide II′), or upon N–H/C exchange [10,11] (amide IIp in the case of the X-Pro bond) [12]. Essentially the same spectrum is seen for a *cis*-peptide bond (amide IIc), [8] because the isomerization alters the amide kinematics, and disrupts the mixing between C–N stretching and N–H bending coordinates. Thus UVRR spectroscopy is quite sensitive to peptide N–H/D exchanges, or to the presence of X-Pro or of *cis*-peptide bonds in a protein.

In this study, we explore additional issues related to peptide UVRR spectroscopy. What are the effects of non-planarity in either *trans*- or *cis*-peptides? And what are the characteristics of inter-peptide interactions? Both of these questions are central to the analysis of protein UVRR spectra. To examine non-planarity effects, we have determined UVRR spectra, in H_2O and D_2O of a series of cyclic amides, with ring sizes (number of atoms) ranging from 4 to 13. For an 8-membered ring, the amide bond is constrained to the *cis* isomer, and decreasing the ring size further pro-

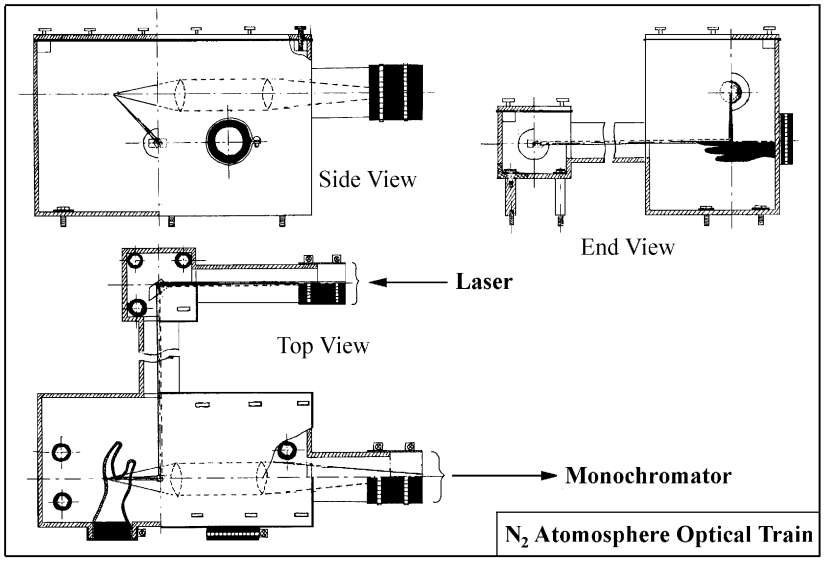

Fig. 1. Design of the plastic enclosure for the far UVRR optical train containing the sampling device and optics. All interfaces were sealed by rubber gaskets. After sample changes, the boxes were purged with nitrogen gas for 30 min at a high flow rate, followed by low flow purging during spectral acquisitions.

duces clear evidence of increasing non-planarity and bond order change. To examine inter-peptide coupling we have recorded UVRR spectra of two cyclic peptides cyclo(Gly–Gly) and cyclo(Gly–Pro). In these molecules the amide IIc coordinates combine into in- and out-of-phase modes, with displaced frequencies. There is also electronic coupling as revealed by the comparison of UVRR excitation profiles (EPs).

2. Materials and methods

2.1. Samples

All chemicals were purchased from Sigma Chemicals and Aldrich Chemicals, and used without further purification.

2.2. UV/Vis measurement

The UV/Vis spectra were collected with a photodiode array-based spectrophotometer (Hewlett-Packard HP 1041A). All spectra were corrected with a blank spectrum of the 5 mM phosphate buffer solution. The sample concentrations were adjusted to give a maximum absorbance between 0.5 and 1.0. In Fig. 6, the spectra are normalized to the same maximum OD within the spectral region 190–250 nm.

2.3. Resonance Raman spectroscopy

Ultraviolet excitation was provided by a Q-switched Nd:YAG laser (1064 nm) with harmonic generation in non-linear optical crystals and Raman shifting in pressurized hydrogen or deuterium gas. The incident light was directed in 135° back-scattering geometry to the sample through a multiple-prism optics system. The scattered light was passed through a quartz wedge polarization scrambler, collected by reflective (Cassegrain) optics, and coupled into a 1.25-m monochromator (Spex 1269) equipped with a single 3600 grooves mm^{-1} holographic grating. The detection system was a photomultiplier tube (Humamatzu, Inc.) with a box-car gating/integrating electronic system (Stanford Research) [13].

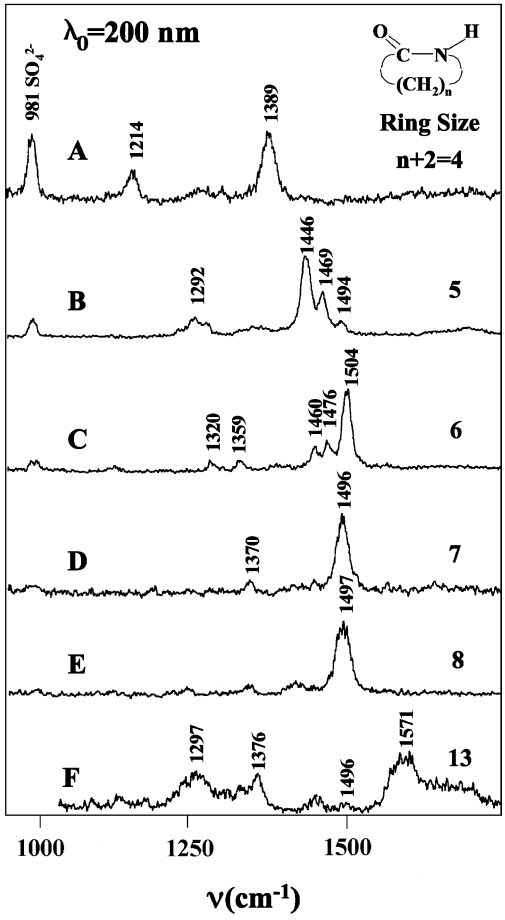

Fig. 2. UVRR spectra obtained with 200 nm excitation for the aqueous solutions (10–30 mM), of cyclic amides with increasing ring size: (a) 2-azaidine; (b) 2-pyrrolidinone; (c) δ-vareloctam; (d) 2-azacyclooctanone; (e) ε-caprolactam and (f) 2-azacyclotridecanone.

For measurements with laser excitation below 200 nm, two modifications to the UVRR system were employed. First, the regular Raman shifter was replaced with a liquid nitrogen-cooled Raman shifter. The cooled Raman shifter, delivered 20–40% more excitation energy for higher orders of anti-stokes shifted outputs. In addition, atmospheric oxygen was eliminated from the entire optical path. From the output of the hydrogen Raman shifter to the spectrometer entrance slit, the optical path was enclosed in two sealed plastic boxes, which were connected by plastic tubes and rubber

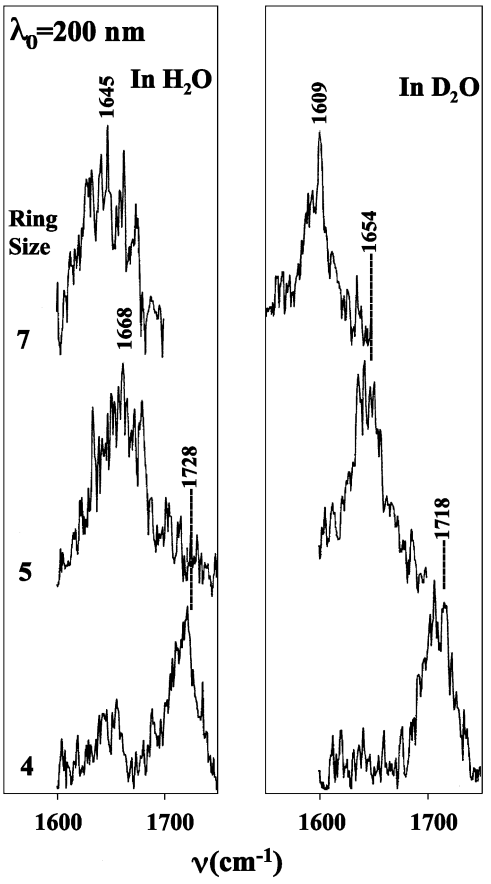

Fig. 3. Two hundred nanometer-excited amide Ic bands in H_2O (right) and D_2O (left) for 4-, 5- and 7-membered cyclic amides. In H_2O, the amide Ic band is partially obscured by overlap with the 1645-cm^{-1} water bending band.

bellows (Fig. 1). Samples and optical components were accessible via the two rubber gloves connected to the boxes. The boxes were purged with N_2 for at least 30 min after each sample change. A N_2 purge was also maintained in the spectrometer.

Spectra were obtained with a thin-film wire-guided sampling device as described previously [13], circulating 3 ml of sample solution via a peristaltic pump. Samples were prepared at concentrations of 10–30 mM in 5 mM phosphate solution buffered at pH 7.4, containing 0.3–0.4 M sodium sulfate as an internal intensity standard. Spectra were collected with 8 cm^{-1} resolution and averaged over 10–25 repeated scans. The spectrum of ethanol was used for frequency calibration using a non-linear fit of multiple frequencies. The frequency accuracy was better than 2 and 4 cm^{-1} for the excitations above and below 200 nm, respectively. The relative intensity calibration factor for each Raman band was obtained from the corresponding intensity readings at the same frequency from a scan of a white-light source (deuterium lamp) under the same experimental conditions.

EPs were obtained through the intensity ratio of the sample Raman bands to that of sulfate. The Raman cross-sections of sulfate below 200 nm

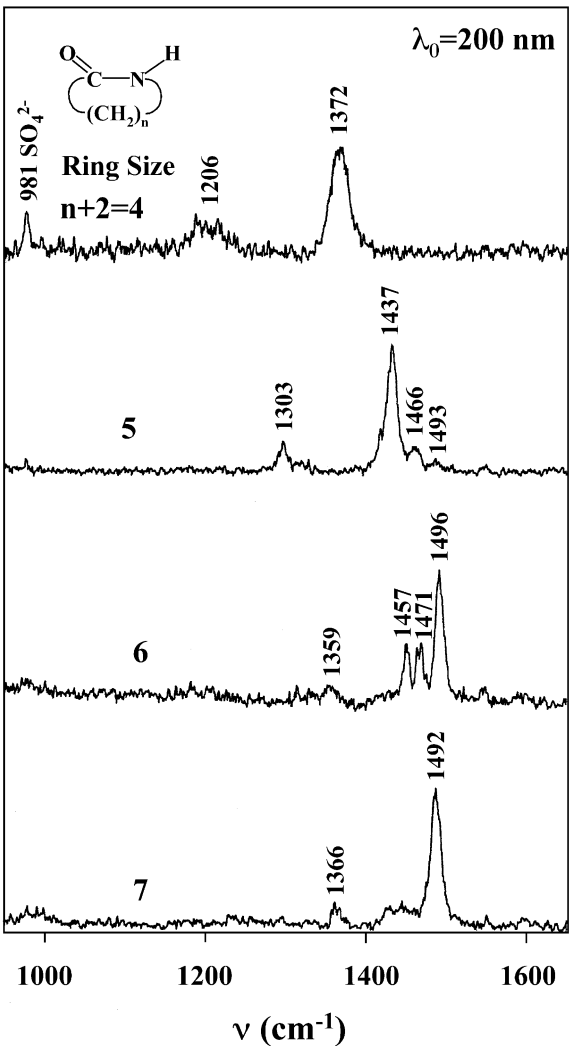

Fig. 4. As Fig. 2, but in D_2O, for the 4- to 7-membered rings.

were extrapolated based on the Raman cross-sections above 200 nm [14] using the Albrecht A term pre-resonance scattering equation [14].

3. Results and discussion

3.1. Ring size and amide frequency

The transition between *trans*- and *cis*-amide configurations is clearly revealed in the UVRR spectra of cyclic amides with large ring sizes (Fig. 2). 2-Azacyclotridecone, which consists of a 13-membered ring, has the standard *trans*-amide spectral signature [6], with comparably strong amide II (1571 cm^{-1}), amide S (1374 cm^{-1}) and amide III (1279 cm^{-1}) bands, while caprolactam, with an 8-membered ring, shows the dramatically simplified *cis*-amide signature [8], with a single strong amide IIc band at 1497 cm^{-1}. This simplification results from unmixing of the N–H bending and C–N stretching coordinates in the amide II and III modes, occasioned by altered kinematics in the *cis* relative to the *trans*-amide conformation [6]. The caprolactam amide II′ frequency is close to that observed for the *cis* isomer of *N*-methylacetamide, produced by photo-excitation [15]. Like wise, 2-azacyclooctanone with a 7-membered ring, has essentially the same amide IIc frequency.

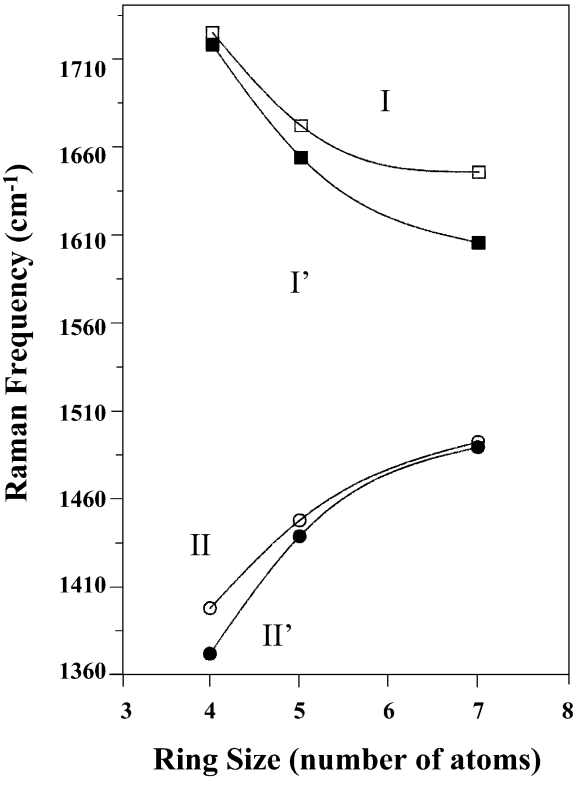

Fig. 5. Anti-correlation of amide Ic and IIc frequencies with increasing ring size, in H_2O (open symbols) and D_2O (filled symbols). The results were obtained from the spectral data in Figs. 2–4.

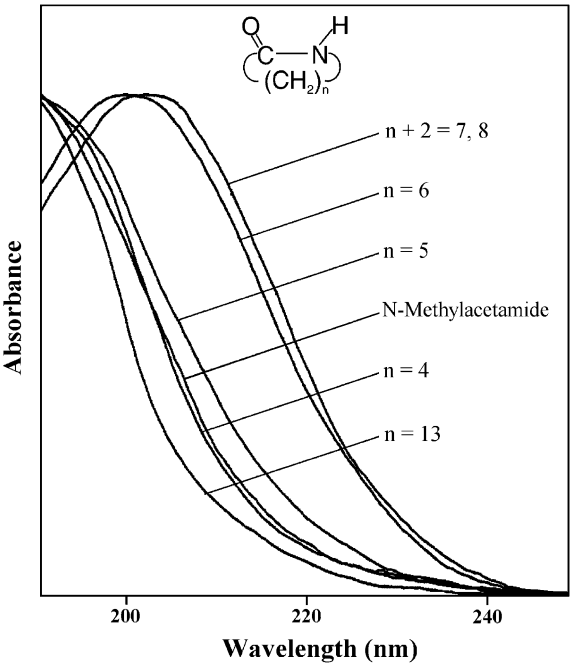

Fig. 6. UV absorption spectra of the indicated amide compounds. The spectra were normalized with respect to the maximum absorbance.

However, when the ring is reduced to 6 or fewer atoms, the amide IIc frequency is strongly perturbed. The 6- and 5-membered rings (δ-verolactam and 2-pyrrolidinone) give multiple UVRR bands in the amide IIc region, attributable to equilibria among several ring conformers (see below), while the 4-membered ring (2-azaidine) gives a strongly down-shifted amide IIc band, at 1389 cm^{-1}. The frequency lowering (>100 cm^{-1}), relative to that for the 7- and 8-membered rings, results from diminution of the C–N bond order, as a result of ring strain, as well as from

altered kinematics [16]. There is a compensating increase in the C=O stretching frequency for the 4-membered ring molecule (Fig. 3), to 1728 cm^{-1} close to the 1735 cm^{-1} C=O stretching frequency of acetone. Although the resonance Raman enhancement of amide Ic is much less than that for amide IIc, careful examination of the 1700 cm^{-1} region reveals that the 1728 cm^{-1} amide Ic band is shifted to 1718 cm^{-1} for the 4-membered molecule in D_2O (Fig. 3), as a result of N–H/D substitution. The amide Ic band is much lower for the 7-membered ring, ~1645 cm^{-1} (where it overlaps with the water bending mode, Fig. 2), and shifts much more, to 1609 cm^{-1}, in D_2O. The position of amide Ic is intermediate, 1668 cm^{-1}, for the 5-membered ring, as is the D_2O shift, to 1654 cm^{-1}.

N–H/D substitution also affects the amide IIc frequency significantly (Fig. 4) for the 4-membered ring, shifting it 26 cm^{-1} from 1398 to 1372 cm^{-1}. Thus the N–H bending contribution is transferred from the amide Ic to the amide IIc mode. In contrast, the amide IIc frequency shifts only 5 cm^{-1} in D_2O for the 7-membered ring. The extent of this shift is intermediate for the 5- and 6-membered rings, for which the main band in the amide IIc region shifts 9 and 8 cm^{-1} in D_2O (Fig. 4). Both the amide Ic and IIc frequencies and isotope shifts vary smoothly with ring size, in an anti-correlated manner (Fig. 5).

Countervailing effects of ring size are seen in the electronic absorption spectra (Fig. 6). The absorption maximum for the first amide $\pi-\pi^*$ transition is ~190 nm for the 13-membered *trans*-amide ring, but it is significantly red-shifted (205–210 nm) for the 6- and 7-membered rings, as a results of the switch to a *cis*-amide conformation. However, the peak shifts to the blue again as the ring size decreases further, and is back to ~190 nm for the 4-membered ring. Thus the electronic interactions responsible for the red-shifted $\pi-\pi^*$ transition in *cis*-amides are offset by the effect of ring strain. As a result the UVRR intensity is significantly lower for both the 13- and 4-membered rings (see noise level in Fig. 1) than for the intermediate ring sizes, which are closer to being in resonance with the 200 nm excitation.

3.2. Conformational equilibrium

For the 5- and 6-membered rings, the relative intensities of the three peaks near 1500 cm^{-1} are sensitive to temperature (Fig. 7), implying that they arise from different species which are in temperature-dependent equilibrium. For the 5-membered ring (left panel, Fig. 7), the minor peaks (1469 and 1493 cm^{-1}) lose intensity relative to the dominant peak (1446 cm^{-1}), whereas for the 6-membered ring the minor peaks (1460 and 1476 cm^{-1}) gain relative intensity at high temperature. We propose that the three peaks in each case correspond to three different non-planar ring conformations, as illustrated in Fig. 8. For the 5-membered ring, the C3, C4 or C5 atoms can be out of the plane of the remaining four atoms, while for the 6-membered ring, the C3 and C4, the C4 and C5 or the C5 and C6 atoms can be out of the plane of the remaining four atoms. In each case, the conformation that maintains the most planar peptide bond is suggested to give rise to highest frequency peak. This would be the 4-*exo* conformation of the 5-membered ring (1493 cm^{-1}) and the 4,5-*exo* conformation of the 6-membered ring (1504 cm^{-1}). The lowest frequency is assigned to the conformation in which the carbonyl C atom is pyramidalized, 3-*exo* (1446 cm^{-1}) and 3,4-*exo* (1460 cm^{-1}), while the middle frequency is assigned to the conformation in which the N-atom is pyramidalized, 5-*exo* (1469 cm^{-1}) and 5,6-*exo* (1476 cm^{-1}). For each of these conformations, the 5-membered ring has the lower frequency, reflecting the greater degree of ring strain.

If these assignments are correct, the temperature dependence indicates that the 6-membered ring conformation with the most planar peptide bond (4,5-*exo*) is the most stable one at low temperature, as would be expected. But for the 5-membered ring it is the C-pyramidalized conformation (3-*exo*) which is the most stable at low temperature. This counterintuitive result must reflect the trade-off between resonance stabilization and severely distorted bond angles when the amide bond is planarized in a 5-membered ring.

3.3. Inter-peptide coupling

In cyclic dipeptides, the amide bonds are *cis*, but their vibrations are mixed in the normal modes.

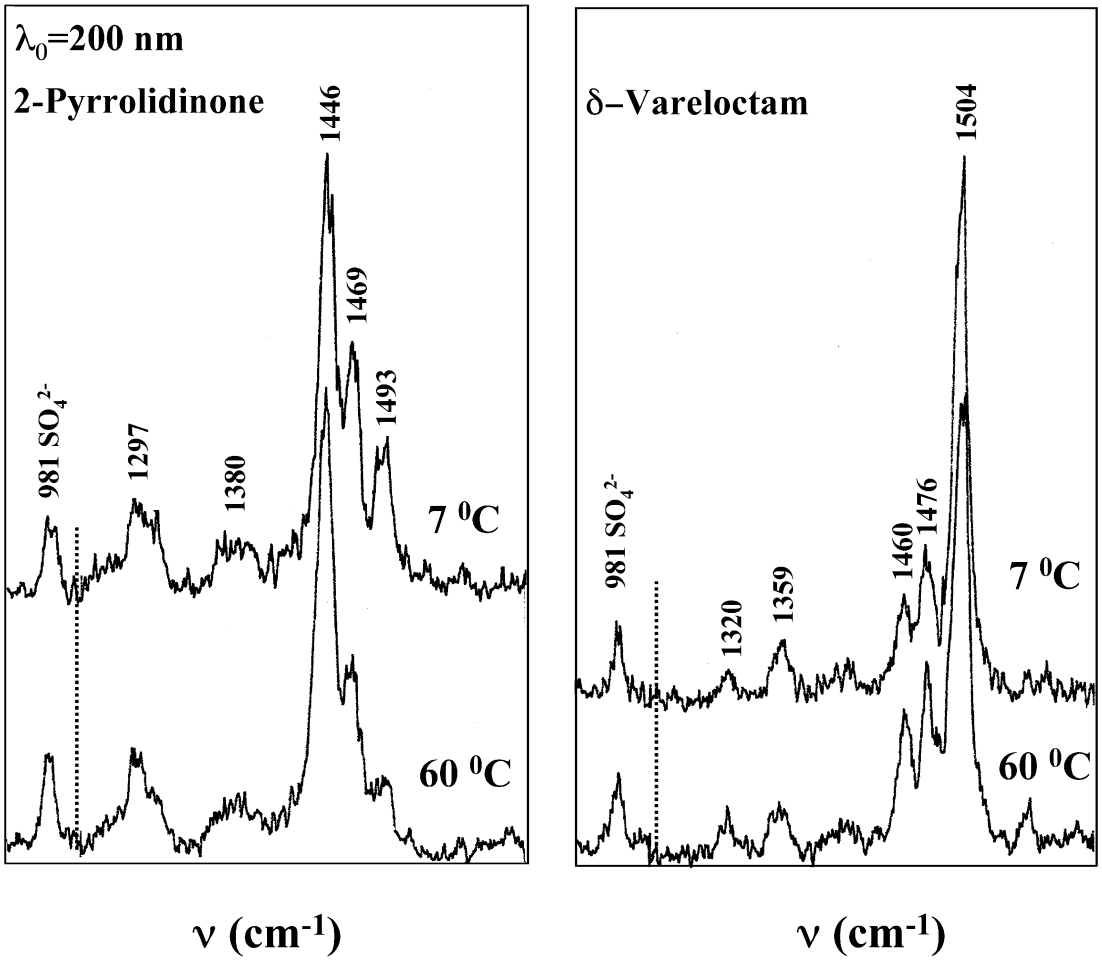

Fig. 7. Temperature dependence of the 200 nm-excited UVRR spectra for the 5- (2-pyrrolidinone) and 6- (δ-verolactam) membered ring cyclic amides.

This effect is illustrated by the UVRR spectra of cyclic glycylproline (cyclo(Gly–Pro)) and glycylglycine (cyclo(Gly–Gly)) (Fig. 9). Cyclo(Gly–Pro) displays two amide IIc bands, at 1475 and 1515 cm^{-1}. The 1515 cm^{-1} band was originally assigned to the X-Pro peptide bond [17], but was reassigned to the X-Gly peptide bond [18], on the basis of its D_2O sensitivity (4 cm^{-1}, see inset). The 1475 cm^{-1} band, which is insensitive to D_2O, was assigned instead to the X-Pro bond [18], since there is no exchangeable H atom on the proline N atom. However, this frequency is 10 cm^{-1} lower than is seen for the X-Pro bond in linear glycylproline (Fig. 9), while the X-Gly frequency is more than 10 cm^{-1} higher than the normal *cis*-amide frequency (e.g. caprolactam, Fig. 9). Thus the two amide oscillators couple via kinematic interactions and transition dipole coupling, producing normal modes with frequencies which are both lower and higher than those displayed by the isolated oscillators.

The frequency difference is even more pronounced for cyclo(Gly–Gly) since the two X-Gly oscillators are degenerate. The normal modes are now in- and out-of-phase combinations of the two oscillators. The in-phase combination gives rise to the UVRR band at 1530 cm^{-1}, significantly higher than the standard *cis*-amide frequency, or even the

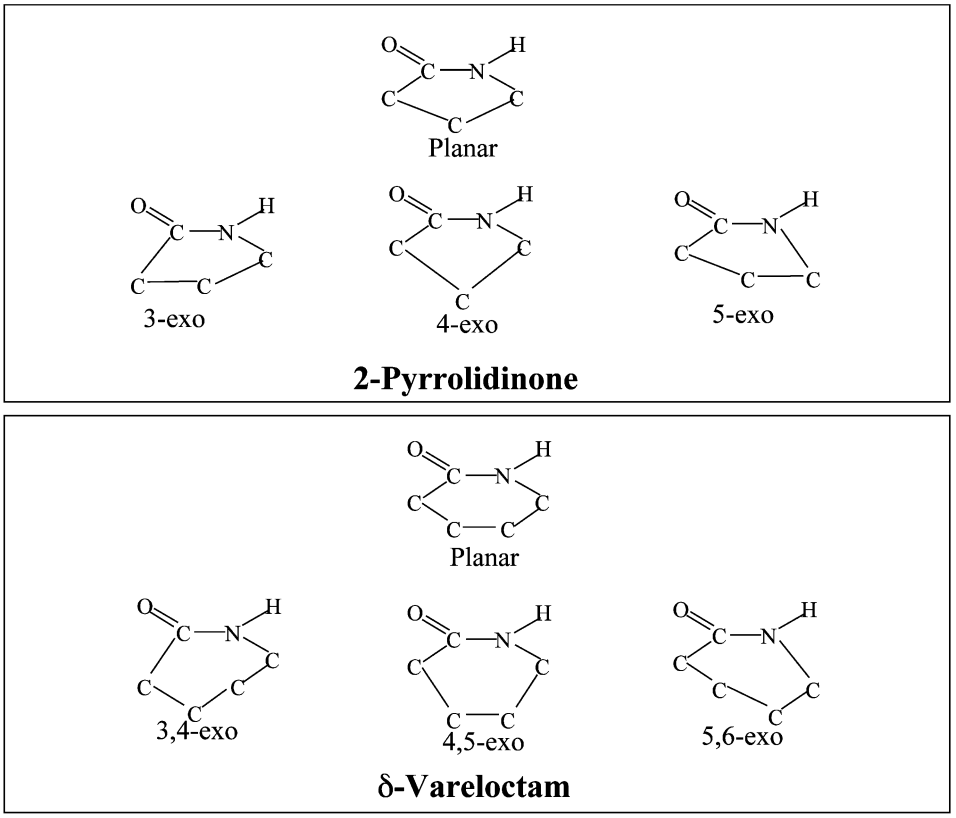

Fig. 8. Structural diagrams for different conformers of the 5- and 6-membered ring amides.

X-Gly frequency in cyclo(Gly–Pro). The out-of-phase combination is not Raman active, since the molecule is centrosymmetric, but is seen in the IR spectrum at 1470 cm^{-1}.

Interestingly, the cyclic dipeptides also show electronic coupling effects in the UVRR EPs (Fig. 10). Amide II of linear glycylproline and amide IIc of caprolactam both show two EP maxima, at 50 and 53–54 kK (top panel, Fig. 9). This double-peaked structure is quite different from the single peak, at ~52 kK which is observed for a secondary *trans*-amide, such as NMA [6]. Apparently, uncoupling of the N–H bending coordinate from the C–N stretching coordinate, either by N–H/C replacement (X-Pro) or by conversion to the *cis* isomer (caprolactam), is accompanied by rearrangement of the $\pi-\pi^*$ energy levels of the amide bond (reflected in their red-shifted UV absorption spectra (Fig. 6)). The amide IIc band (in-phase mode—see above) of cyclo(Gly–Gly) (bottom panel) exhibits a broad EP, rising to a cross-section which is about double that of the caprolactam maxima, consistent with additive behavior of the two X-Gly transition dipoles.

Both behaviors are seen for the cyclo(Gly–Pro) EP's (middle panel), double humped for the X-Pro amide IIc and a broad single maximum for the X-Gly amide IIc. The cross-sections are much lower and higher, respectively, relative to caprolactam, for X-Pro and X-Gly. (This is why the 1476 cm^{-1} X-Pro bond was missed in the original UVRR study [17].) Thus, the two amide oscillating dipoles add up in the in-phase mode (X-Gly) and nearly cancel in the out-of-phase mode (X-Pro).

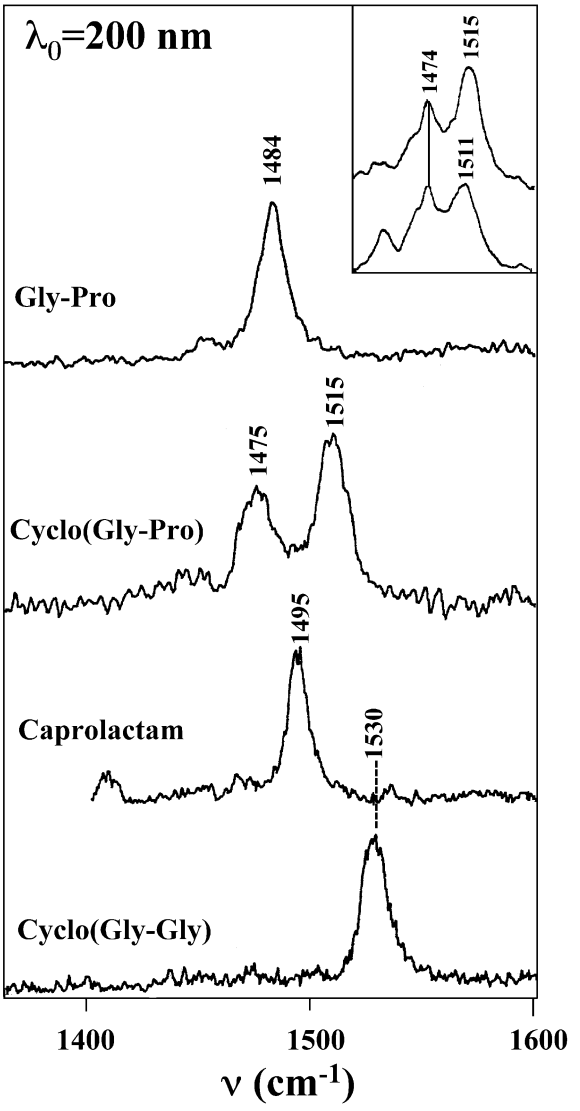

Fig. 9. Two hundred nanometer-excited UVRR spectra in the amide IIc region for the indicated amides. The inset shows the D_2O shift for cyclo(Gly–Pro).

This behavior is the same as that observed for cyclo(Gly–Gly), for which symmetry requires that the out-of-phase cancellation be complete.

4. Conclusions

Placing the amide bond in a 7- or 8-membered ring constrains it to the *cis* isomer, but the bond remains planar. Reducing the ring size further induces non-planarity, which lowers the amide IIc and raises the amide Ic frequency, as a result of localization of the double bond character to the carbonyl group. The shifts are large, over 100 and over 80 cm^{-1}, respectively, for amide IIc and Ic in the case of the 4-membered ring, comparing with the unconstrained ring structure. Although, similar effects have yet to be documented for *trans*-amides (molecules with non-planar *trans*-amide bonds being difficult to produce), one can speculate that the large widths of the amide vibrational bands that are commonly seen in proteins may result from small non-planar distortions of the amide bonds along the folded polypeptide chain.

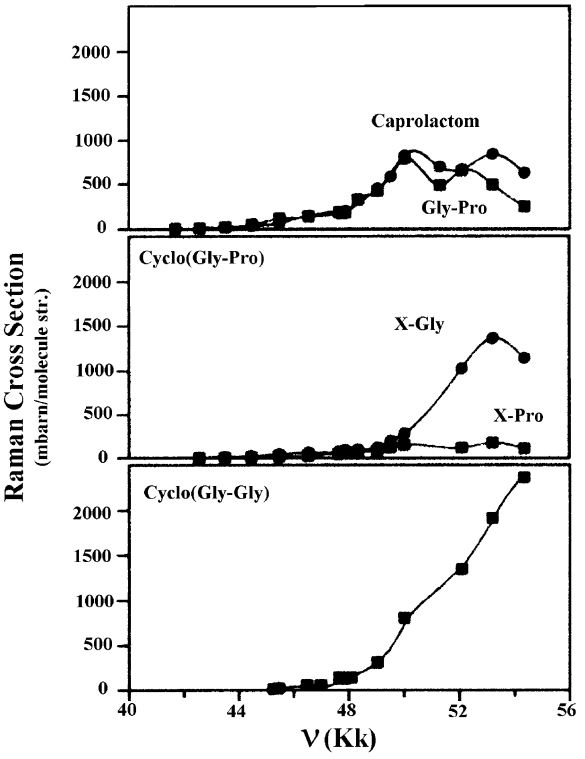

Fig. 10. Amide IIc EPs for the indicated amides: top, caprolactam and the X-Pro bond of linear Gly–Pro; middle, X-Gly and X-Pro bonds of cyclo(Gly–Pro), bottom, X-Gly bond of cyclo(Gly–Gly).

There is substantial inter-amide coupling in cyclic dipeptides, both kinematically and electronically. These effects have not previously been studied in peptides of constrained geometry.

Acknowledgments

This work gratefully acknowledges the support by NIH Grant GM25156. We thank Alex Pevsner for help in preparing the manuscript.

References

[1] (a) A. Ianoul, A. Mikhonin, I.K. Lednev, S.A. Asher, UV resonance Raman study of the spatial dependence of alpha-helix unfolding, J. Phys. Chem. A 106 (2002) 3621–3624
(b) I.K. Lednev, A.S. Karnoup, M.C. Sparrow, S.A. Asher, Transient UV Raman spectroscopy finds no crossing barrier between the peptide alpha-helix and fully random coil conformation, J. Am. Chem. Soc. 123 (2001) 2388–2392.

[2] I. Harada, H. Takeuchi, in: R.J.H. Clark, R.E. Hester (Eds.), Spectroscopy of Biological Systems, Wiley, Chichester, 1986, p. 113.

[3] B.S. Hudson, L.C. Mayne, in: T.G. Spiro (Ed.), Biological Application of Raman Spectroscopy, vol. 2, Wiley–Interscience, New York, 1987, Chapter 3.

[4] J.C. Austin, K.R. Rodgers, T.G. Spiro, Protein-structure from ultraviolet resonance Raman-spectroscopy, Method. Enzymol. 226 (1993) 374–396.

[5] Y. Wang, R. Purrello, S. Georgiou, T.G. Spiro, UVRR spectroscopy of the peptide-bond 2. Carbonyl H-bond effects on the ground-state and excited-state structures of *N*-methylacetamide, J. Am. Chem. Soc. 113 (1991) 6368–6377.

[6] Y. Wang, R. Purrello, T. Jordan, T.G. Spiro, UVRR spectroscopy of the peptide-bond 1. Amide-S, a non-helical structure marker, is a C-alpha-H bending mode, J. Am. Chem. Soc. 113 (1991) 6359–6368.

[7] S.A. Asher, A. Ianoul, G. Mix, et al., Dihedral psi angle dependence of the amide III vibration: a uniquely sensitive UV resonance Raman secondary structural probe, J. Am. Chem. Soc. 123 (2001) 11775–11781.

[8] T. Jordan, T.G. Spiro, UV resonance Raman-spectroscopy of *cis*-amides, J. Raman Spectrosc. 26 (1995) 867–876.

[9] T. Miyazawa, T. Shimanouchi, S.J. Mizushima, Normal vibrations of *N*-methylacetamide, J. Phys. Chem. 29 (1958) 611–616.

[10] T. Jordan, T.G. Spiro, Enhancement of C-alpha hydrogen vibrations in the resonance Raman-spectra of amides, J. Raman Spectrosc. 25 (1994) 537–543.

[11] D.S. Caswell, T.G. Spiro, Proline signals in ultraviolet resonance Raman spectra of proteins: *cis–trans* isomerism in polyproline and ribonuclease A, J. Am. Chem. Soc. 109 (1986) 2796.

[12] T. Jordan, I. Mukerji, Y. Wang, T.G. Spiro, UV resonance Raman spectroscopy and hydrogen bonding of the proline peptide bond, J. Mol. Struct. 379 (1996) 51–64.

[13] S.P.A. Fodor, R.P. Rava, R.A. Copeland, T.G. Spiro, H-2 Raman-shifted Yag laser ultraviolet Raman spectrometer operating at wavelengths down to 184 nm, J. Raman Spectrosc. 17 (1986) 471–475.

[14] J.M. Dudik, C.R. Johnson, S.A. Asher, Wavelength dependence of the preresonance Raman cross-sections of CH_3CN, SO_4^{2-}, ClO_4^-, and NO_3^-, J. Chem. Phys. 82 (1985) 1732–1740.

[15] Y. Wang, R. Purrello, T.G. Spiro, UV photoisomerization of *N*-methylacetamide and resonance Raman enhancement of a new conformation—sensitive amide mode, J. Am. Chem. Soc. 111 (1989) 8274–8276.

[16] N.B. Colthup, M.K. Orloff, Strained ring carbonyl force constants from molecular-orbital calculations, Chem. Phys. Lett. 19 (1973) 298–300.

[17] L.C. Mayne, B.S. Hudson, Selective enhancement of proline Raman signals with ultraviolet excitation, J. Phys. Chem. 91 (1987) 4438–4440.

[18] H. Takeuchi, I. Harada, Ultraviolet resonance Raman-spectroscopy of X-proline bonds—a new marker band of hydrogen-bonding at the imide C=O site, J. Raman Spectrosc. 21 (1990) 509–515.